Paris saponin H inhibits the proliferation of glioma cells through the A1 and A3 adenosine receptor-mediated pathway

LINLIN BI, YANG LIU, QIAN YANG, XUANXUAN ZHOU, HUA LI,
YANG LIU, JIE LI, YUNYANG LU and HAIFENG TANG

Department of Chinese Materia Medica and Natural Medicines, Air Force Medical University,
Xi'an, Shaanxi 710032, P.R. China

Abstract. *Paris* saponin H (PSH) is a type of steroid saponin derived from Rhizoma Paridis (RP; the rhizome of *Paris*). In our previous studies, saponins from RP exerted antiglioma activity *in vitro*. However, the effects of PSH on glioma have not been elucidated. The aim of the present study was to evaluate the effects of PSH on U251 glioblastoma cells and elucidate the possible underlying mechanism. The cells were treated with PSH at various concentrations for 48 h, and the cell viability, invasion, apoptosis and cycle progression were assessed using specific assay kits. The activation of Akt, 44/42-mitogen-activated protein kinase (MAPK) and the expression levels of A1 adenosine receptor (ARA1) and ARA3 were assessed by western blotting. The results demonstrated that PSH inhibited cell viability, migration and invasion, and induced apoptosis. Treatment of U251 cells with PSH induced the upregulation of p21 and p27, and the downregulation cyclin D1 and S-phase kinase associated protein 2 protein expression levels, which induced cell cycle arrest at the G1 phase. The results also demonstrated that PSH inhibited the expression of ARA1, and the agonist of ARA1, 2-chloro-N6-cyclopentyladenosine, reversed the effects of PSH. Hypoxia induced increases in the ARA3, hypoxia-inducible factor-1α (HIF-1α) and vascular endothelial growth factor (VEGF) protein expression levels, which were associated with the activation of the Akt and P44/42 MAPK pathways. Compared with the hypoxia group, PSH inhibited the expression levels of ARA3, HIF-1α and VEGF, as well as the phosphorylation levels of Akt and 44/42 MAPK, and repressed HIF-1α transcriptional activity. Furthermore, the results demonstrated that PSH inhibited the expression of HIF-1α by inhibiting the phosphorylation of Akt and 44/42 MAPK mediated by ARA3. Taken together, these results suggested that PSH reduced U251 cell viability via the inhibition of ARA1 and ARA3 expression, and further inhibited Akt and 44/42 MAPK phosphorylation, induced apoptosis and cell cycle arrest.

Introduction

Glioblastoma is one of the most malignant types of brain cancer, characterized by high recurrence and mortality rates, and a low cure rate (1,2). Due to the invasive growth of glioma, tumor tissue cannot be completely removed with surgery, and it can easily relapse *in situ*, making it difficult to cure. The prognosis of patients with glioblastoma is unsatisfactory, with an annual survival rate <30% and a 5-year survival rate <5% in the United States between 2000 and 2014 (3,4). The resistance of glioma chemotherapeutic drugs is the leading cause of treatment failure (5). Traditional chemotherapy agents, such as carmustine, cisplatin and teniposide, are commonly used; however, they are only ~20% efficient, with the efficiency of the newest drug, temozolomide, at only 35% (6). Therefore, developing new strategies and drugs to effectively inhibit glioma growth has become one of the main research goals of scientists worldwide.

A number of studies have demonstrated that extracellular adenosine signaling is associated with glioma cell proliferation, migration, invasion and mortality in animal models (7). Although the concentration of adenosine in the extracellular fluid of glioma tissue is in the micromolar range, it is sufficient to activate all known adenosine receptor subtypes (A1, A2A, A2B and A3) (8). Among them, A2A and A2B receptors are mainly distributed on epithelial and a variety of immune cells, and the A1 and A3 adenosine receptors are distributed on the tumor cell membrane and serve a key role in tumor cell proliferation and invasion (9). Under hypoxic and normal oxygen environments, the same adenosine receptor may exert different biological effects (10). Due to the regulatory effects of adenosine receptors and their downstream signaling pathways, chemical compounds or drugs that affect these receptor may inhibit the proliferation and angiogenesis of glioma cells.

In our previous studies, a number of saponins (e.g. saponin 6 of *Anemone taipaiensis*) with antiglioma activity were isolated and identified from various medicinal plants, and the feasibility of saponin treatment on malignant

Correspondence to: Professor Haifeng Tang, Department of Chinese Materia Medica and Natural Medicines, Air Force Medical University, 127 Changle road, Xi'an, Shaanxi 710032, P.R. China
E-mail: tanghaifeng71@163.com

glioma was determined by interstitial chemotherapy (11-13). Rhizoma Paridis (RP; the rhizome of *Paris*) has a wide range of medicinal activities, including anticancer, and has been used for the treatment of lung cancer, brain tumors and malignant lymphomas (14). In previous studies, saponins from RP showed good effects in inhibiting tumor effects, including inducing apoptosis and cell cycle arrest, inhibiting angiogenesis and increasing immunity (15,16). *Paris* saponin H (PSH), a steroid saponin component of RP, shares similar characteristics with Polyphyllin VII, Polyphyllin D and *Paris* Saponin II (17). Polyphyllin VII and Polyphyllin D have been demonstrated to exert their antiglioma effects *in vitro* by inducing apoptosis (18,19). *Paris* Saponin II serves an anti-angiogenetic role through reducing the levels of VEGF and blocking the activity of VEGFR2 (20). Total steroidal saponins extracted from the RP have been demonstrated to activate adenosine receptors in rat platelets, and several saponins (including N6-cyclohexyladenosine and 8-cyclopentyl1, 3-dipropyl-2,3-(N)-xanthine) exert inhibitory effects on A1 and A3 adenosine receptors (21,22).

However, the mechanism of PSH against glioma remains unclear. Based on the aforementioned previous experiments, we hypothesized that PSH may bind to the A1 and A3 adenosine receptors on glioma cell membranes, inhibit their downstream signaling pathways, promote tumor cell apoptosis and inhibit glioma growth. On the other hand, the inhibition of the A3 receptor activation may reduce hypoxia-inducible factor-1α (HIF-1α) synthesis, which may in turn inhibit glioma angiogenesis and cell proliferation.

Materials and methods

Chemicals and reagents. PSH (purity, 98%) was obtained from the Department of Natural Medicine, School of Pharmacy, Fourth Military Medical University. Cell Counting Kit-8 (CCK-8) was purchased from Shanghai 7Sea PharmTech Co. Ltd. Human astrocytoma U251 cells were purchased from the Cell Bank of Type Culture Collection of The Chinese Academy of Sciences. RIPA buffer, CHAPS buffer, caspase-3 (cat. no. C1116) and caspase-9 (cat. no. C1158) activity assay kits were purchased from Beyotime Institute for Biotechnology. VEGF ELISA kit (cat. no. PDVE00) was purchased from R&D Systems, Inc. Dulbecco's modified Eagle's medium (DMEM) and fetal bovine serum (FBS) were purchased from Gibco; Thermo Fisher Scientific, Inc. The Annexin V-FITC/PI staining kit was purchased from Nanjing Jiancheng Bioengineering Institute. The primary antibodies against HIF-1α (cat. no. 36169), VEGF (cat. no. 2463), MAP kinase kinase 1/2 (MEK1/2; cat. no. 8727), phosphorylated (P-)MEK1/2 (cat. no. 9154), P38 mitogen-activated protein kinase (MAPK; cat. no. 8690), P-P38 MAPK (cat. no. 4511), Akt (cat. no. 4691), P-Akt (cat. no. 4060), P44/42 MAPK (cat. no. 4695), P-P44/42 MAPK (cat. no. 4370), P27 (cat. no. 3686) and CDK4 (cat. no. 12790) were purchased from Cell Signaling Technology, Inc. The peroxidase-conjugated anti-rabbit (cat. no. BA1056) and anti-mouse (cat. no. BA1050) secondary antibodies were purchased from Wuhan Boster Biological Technology, Ltd. LY294002 (cat. no. 19-142), U0126 (cat. no. 19-147), 2-Chloro-N6-cyclopentyladenosine (CCPA; cat. no. 37739-05-2), 2-chloro-N6-(3-iodobenzyl)

adenosine-50-N-methylcarboxamide (CI-IB-MECA; cat. no. 163042-96-4), 9-chloro-2-(2-furanyl)-5-(phenylacetyl) amino-(1,2,4) triazolo (1,5-c) quinazoline (MRS1220; cat. no. 183721-15-5) and other reagents for buffer preparations were purchased from Sigma-Aldrich; Merck KGaA.

Cell culture. U251 cells were cultured in DMEM supplemented with 10% FBS, 100 U/ml streptomycin and 100 μg/ml penicillin at 37°C with 5% CO_2. The culture medium was changed every other day, and the cells were subcultured when 90% confluence was reached. The cells were inoculated on suitable culture plates specific to each assay and treated with 25, 50 or 100 μg/ml PSH for 72 h at 37°C. The cells in the control group were cultured in normal medium for the same amount of time. Treatment with LY294002 (20 μM), U0126 (20 μM), CCPA (20 nM), CI-IB-MECA (15 μM) and MRS1220 (1 μM) were performed simultaneously with PSH treatment.

Cell viability. U251 cells were seeded into 96-well plates at a density of $5x10^5$ cells/well and cultured for 24 h, followed by continuous culture with PSH for 72 h at 37°C. Cell viability was examined by CCK-8 assay. Briefly, after the treatments, 10 μl CCK-8 solution was added into each well and incubated at 37°C for 4 h, and the absorbance was measured at 455 nm. The cells in the control group were cultured in normal medium. Data are presented as the fold-change relative to the control group.

Apoptotic rate measurement. The PSH-induced apoptosis rate of U251 cells was determined using Annexin V-FITC/PI staining. U251 cells were seeded into 6-well plates at a density of $1x10^6$ cells/well and cultured for 24 h at 37°C. Following the aforementioned treatments, the cells were washed with PBS, trypsinized with 0.125 g/l trypsin, centrifuged at 800 x g for 5 min at room temperature and collected. The cells were resuspended in 100 μl 1X binding buffer, and 5 μl Annexin V-FITC and 5 μl PI were added to each well and incubated for 15 min at 37°C in the dark. Subsequently, 400 μl binding buffer was added, and apoptosis was analyzed on a FACSCalibur flow cytometer with BD Accuri™ C6 software (both BD Biosciences). A total of $1x10^4$ cells were collected per well, and early and late apoptotic cells were recorded.

Cell cycle analysis. The inhibitory effects of PSH on cell proliferation were measured by flow cytometry. Following the aforementioned treatments, U251 cells were collected and fixed with 70% ethanol at 4°C for 2 h. Following centrifugation (800 x g for 5 min at 4°C), the cells were resuspended in RNase A solution and 0.02 mg/ml PI (Sigma-Aldrich; Merck KGaA), and incubated for 30 min at 4°C. The fluorescence of $1x10^4$ cells was recorded by a FACSCalibur C6 flow cytometer (BD Biosciences) and analyzed by ModFit software (Verity Software House).

Invasion assay. To determine the effects of PSH on cell invasiveness *in vitro*, Matrigel Basement Membrane Matrix (Corning, Inc.)-coated Transwell inserts (Costar; Corning, Inc.) were used. The Transwell inserts were coated with 0.8 mg/ml Matrigel at 37°C for 2 h, and cells were seeded at a density of $1x10^6$ and treated with various concentrations of

PSH. Following incubation for 72 h at 37˚C, the non-invasive cells were removed by a cotton swab, and the cells that passed through the membrane into the lower wells were fixed with 5% glutaraldehyde at 37˚C for 30 min and stained with 0.1% crystal violet at 37˚C for 30 min. Images in five random fields per sample were captured using a light microscope, and the cells were counted by ImageJ software (version 1.42, National Institutes of Health). The results were expressed as the percentage of total cells in the lower and upper wells.

Wound healing assay. To investigate the effects of PSH on cell migration, a wound healing assay was performed. Cells were seeded into 6-well plates at 1×10^6 cells/ml, and cultured until a confluent monolayer was formed. The cell surface was wounded by a 200-μl pipette tip. PBS was used to remove the cells from the wound area, and the cells were treated with different doses of PSH in DMEM containing 1% FBS; the serum concentration was based on previous studies (23,24). Images of the wound areas were captured by an inverted microscope (x200 magnification) at the start of the experiment (0 h) and following treatment for 72 h. For each experiment, five replicates were performed, and the experiment was repeated three times. The gap width was calculated using ImageJ software (version 1.42), and the width was expressed in arbitrary units. The wound healing rate was calculated as follows: Wound healing (%)=(1-B/A) x 100%, where A is the gap width at 0 h, and B is the gap width at 72 h.

Caspase activation analysis. To determine the caspase activity, 5×10^5 cells were seeded in 6-well plates and treated as aforementioned. Caspase-3 and 9 activation was measured using specific kits, and the direction and absorption values were recorded at 405 nm using a microtiter plate reader (Bio-Rad Laboratories, Inc.).

20S proteasome enzymatic activity analysis. To avoid affecting the enzymatic activity of the proteasome, 0.5% CHAPS buffer was used to prepare the total cellular protein lysate. The proteasome activity was determined in the total protein lysates using a Proteasome 20S Activity Assay kit (cat. no. ab112154; Abcam) according to the manufacturer's instructions. The fluorescence intensity was measured at the excitation/emission wavelengths of 490/525 nm using a VICTOR X2 fluorescent microplate reader (PerkinElmer, Inc.).

Immunoblotting. Following the aforementioned treatments, the cells were harvested and homogenized in RIPA buffer at 4˚C for 30 min. The protein concentration was determined by the BCA assay (Beyotime Institute of Biotechnology). Protein (30 μg) from each sample was resolved by 10% SDS-PAGE, followed by transfer to a PVDF membrane (Bio-Rad Laboratories, Inc.). Following blocking with 5% non-fat dry milk at 37˚C for 30 min, the membranes were probed with anti-HIF-α (1:1,000), anti-VEGF (1:1,000), anti-P27 (1:1,000), anti-CDK4 (1:1,000), anti-cleaved caspase-9 (1:1,000), anti-cleaved caspase 3 (1:1,000), anti-Akt (1:1,000), anti-P-Akt (1:1,000), anti-P38 (1:1,000), anti-P-P38 (1:1,000), anti-p44/42 MAPK (1:1,000), anti-P-p44/42 MAPK (1:1,000), anti-ARA1 (1:200), anti-ARA3 (1:200) and anti-GAPDH (1:1,000) primary antibodies at 4˚C overnight. Subsequently, the membranes were washed with PBS + 1% Tween-20 three times and incubated with horseradish peroxidase-conjugated anti-rabbit or mouse IgG (1:5,000) at 37˚C for 1 h. The signals were visualized using an ECL Plus western blot detection system. The grayscale values of the bands were calculated using Image J software (version 1.42) and presented as the fold-change relative to the control group.

Statistical analysis. All experiments were repeated three times, and the data are presented as the mean ± SD. The differences between two groups were evaluated by either one-way analysis of variance followed by the Dunnett's or Bonferroni post hoc test using using GraphPad Prism 7.0 (GraphPad Software, Inc.). P<0.05 was considered to indicate a statistically significant difference.

Results

PSH inhibits U251 cell viability. To evaluate the inhibitory effects of PSH on U251 cells, the cells were treated with a range concentrations of PSH for various durations, and the cell viability was measured by CCK-8 assay. As presented in Fig. 1A, PSH inhibited the viability of U251 cells by ~60% at a concentration of 100 μg/ml. Therefore, in subsequent experiments, 25, 50 and 100 μg/ml PSH was used to study the concentration-dependent effects.

To evaluate the inhibitory effects of PSH on U251 migration and invasion, wound healing and Transwell assays were carried out. As demonstrated in Fig. 1B, PSH significantly inhibited cell migration. In the invasion assay, a large number of control cells passed through the filter into the lower wells; 25 μg/ml PSH exhibited an inhibitory effect, but there was no significant difference in the invasive cell number compared with that in the control group (Fig. 1C and D). PSH at 50 and 100 μg/ml significantly decreased the number of cells in the lower wells, suggesting that PSH exerted an inhibitory effect on U251 cell invasion.

PSH induces apoptosis in U251 cells. To evaluate the effects of PSH on apoptosis, Annexin V-FITC/PI staining was used. Treatment with PSH increased the apoptotic rate of U251 cells compared with that in the control group. The caspase 3 and caspase 9 activation analysis demonstrated that 50 and 100 μg/ml PSH significantly increased the activation of caspase 3 and caspase 9 compared with that in the control group (Fig. 2B and C). Western blotting results also revealed that compared with those in the control group, PSH treatment significantly increased the protein expression levels of cleaved caspase 3, cleaved caspase 9, Bcl2-associated X protein and cytochrome *c*. Furthermore, the expression levels of the anti-apoptotic protein Bcl-2 were reduced in all PSH-treated groups compared with those in the control group. These results suggested that PSH induced apoptosis in U251 cells.

PSH induces cell cycle arrest at the G1 phase in U251 cells. To further evaluate whether the inhibitory effects of PSH on cell proliferation were associated with the induction of cell cycle arrest, PI staining was used and analyzed by flow cytometry. As demonstrated in Fig. 3A, PSH induced cell accumulation at the G1 phase, and a reduction at the S and G2
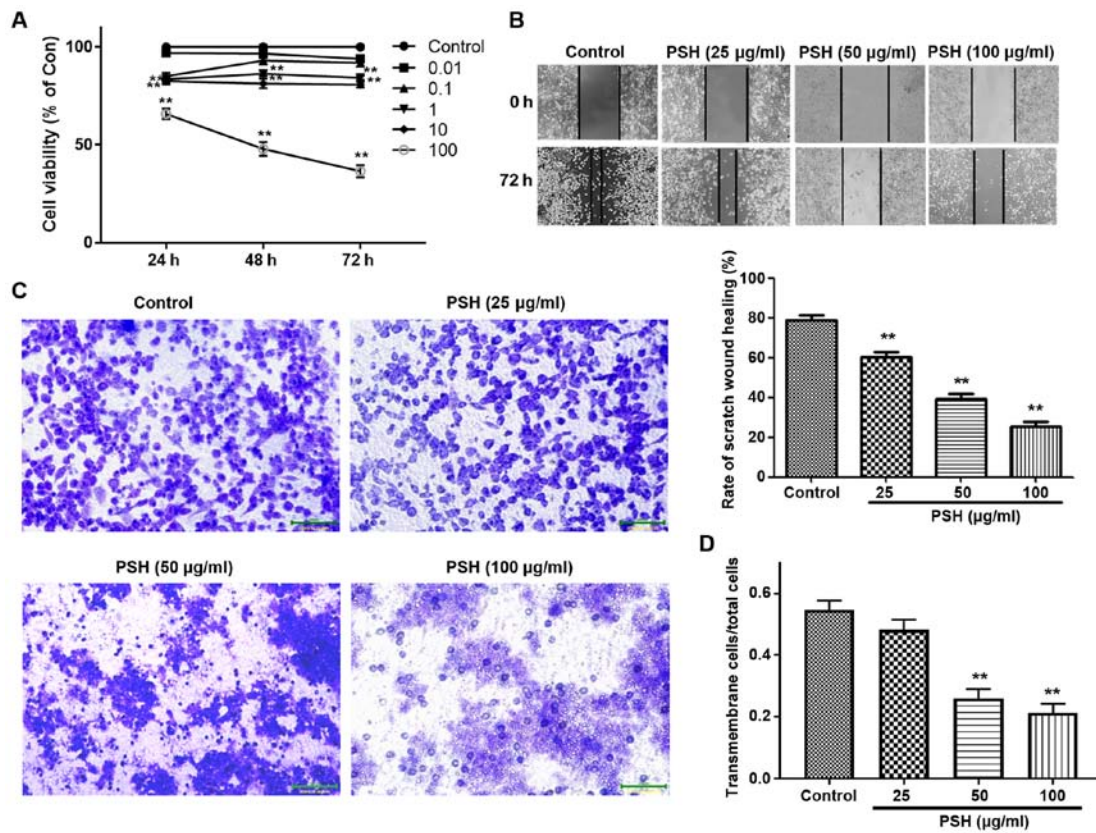
Figure 1. Effects of PSH on U251 cell viability, migration and invasion. (A) Cells were treated with 0.01, 0.1, 1, 10 and 100 μg/ml PSH for 24, 48 and 72 h, and the cell viability was measured by Cell Counting Kit-8 assay. (B) Effects of PSH on cell migration. After confluence was reached, cells were treated with 25, 50 and 100 μg/ml PSH, and the wound healing assay was performed. (C) Effects of PSH on U251 cell invasion. (D) Quantitative data of the cell invasion assay results. **P<0.01 vs. control. PSH, *Paris* saponin H; Con, control.

phases compared with the control group. The western blotting results also revealed that compared with those in the control group, treatment with 25, 50 or 100 μg/ml PSH increased the protein expression levels of P21 and P27, and inhibited those of cyclin D1 and S-phase kinase associated protein 2 (Skp2) (P<0.01). These results suggested that PSH induced cell cycle arrest at the G1 phase in U251 cells.

PSH induces cell cycle arrest via ARA1. To investigate whether the PSH-induced cell cycle arrest in U251 cells was ARA1-dependent, the expression of ARA1 was determined by western blotting (Fig. 4A). Following 48-h treatment with 25, 50 or 100 μg/ml PSH, the protein expression levels of ARA1 were significantly decreased compared with those in the control group. To clarify the role of ARA1, the ARA1 agonist CCPA was used. As demonstrated in Fig. 4B, the effects of PSH on the expression levels of ARA1, P27 and cyclin D1 were reversed by CCPA. The PSH-induced cell cycle arrest was also abolished by CCPA (Fig. 4C). These results suggested that the PSH-induced cell cycle arrest was partly dependent on ARA1.

PSH attenuates HIF-1α and VEGF expression in U251 cells under hypoxia. The effects of PSH on the expression of HIF-1α and VEGF were analyzed in U251 cells under hypoxic conditions. The expression levels of HIF-1α and VEGF were significantly increased following exposure to hypoxia for 48 h compared with those under normoxic conditions. However, treatment with 25, 50 or 100 μg/ml PSH significantly reversed

the effects of hypoxia on HIF-1α and VEGF expression levels (Fig. 5A). Next, the effects of PSH on the HIF-1α transcriptional activity were examined; as demonstrated in Fig. 5B, hypoxia induced a significant increase in HIF-1α transcriptional activity compared with that under normoxia. Treatment with 25, 50 or 100 μg/ml PSH resulted in a significant reduction of HIF-1α transcriptional activity compared with that in the hypoxia group The production of VEGF was also analyzed. Hypoxia significantly induced VEGF secretion compared with that under normoxic conditions, and PSH inhibited this effect (Fig. 5C). Subsequently, 20S proteasome activity in U251 cells was measured following PSH treatment. The results demonstrated that treatment with 25, 50 or 100 μg/ml PSH resulted in a significant reduction in U251 cell proteasome activity, which compared with that in the hypoxia group (Fig. 5D).

PSH inhibits the PI3K/Akt and MAPK signaling pathways in U251 cells under hypoxia. To verify the inhibitory effects of PSH on the expression of HIF-1α and VEGF, as well as the potential roles of the PI3K/Akt and MAPK signaling pathways in the underlying mechanism, the effects of PSH on these pathways were determined. As demonstrated in Fig. 6A, the phosphorylation levels of Akt and 44/42 MAPK in U251 cells were upregulated by hypoxia compared with those in the control group, but inhibited by 25, 50 or 100 μg/ml PSH compared with those in the hypoxia group. Furthermore, the specific PI3K/Akt inhibitor LY294002 and the P44/42 MAPK
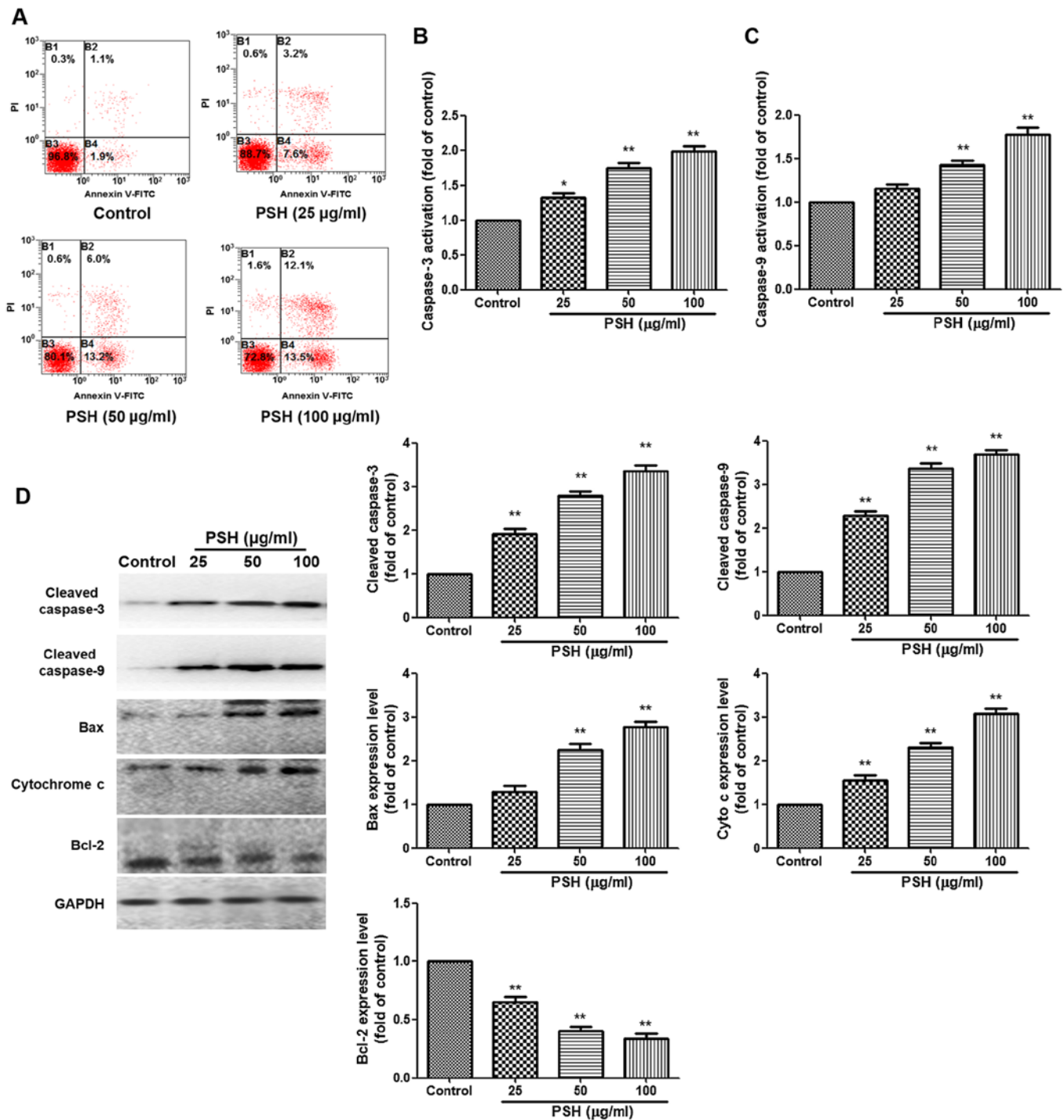
Figure 2. Effects of PSH on U251 cell apoptosis. (A) The rate of cell apoptosis was measured by Annexin V-FITC/PI staining and flow cytometry. (B and C) The activity levels of (B) caspase-3 and (C) caspase-9 were determined by ELISA. (D) Western blotting was used to determine the protein levels of cleaved caspases-3 and 9, Bax, cytochrome c and Bcl-2. The results are presented as the fold-change relative to the control group. Experiments were repeated three times, and the data are presented as the mean ± SD. *P<0.05 and **P<0.01 vs. control group. PSH, *Paris* saponin H.

inhibitor U0126 were used to clarify these effects. As presented in Fig. 6B, compared with those in the PSH treatment group, LY294002 and U0126 inhibited the phosphorylation levels of PI3K/Akt and P44/42 MAPK, respectively. In addition, LY294002 and U0126 abolished the inhibitory effects of PSH on the protein expression levels of HIF-1α and VEGF in U251 cells. These results indicated that the PI3K/Akt and MAPK signaling pathways were involved in the effects of PSH on HIF-1α and VEGF expression.

PSH decreases HIF-1α expression via ARA3 inactivation. To determine whether ARA3 was involved in PSH-induced cytotoxicity, the protein expression levels of ARA3 were analyzed using western blotting. As demonstrated in Fig. 7A, treatment with 25, 50 or 100 μg/ml PSH decreased ARA3 expression levels compared with those in the hypoxia group. To confirm the effects of ARA3 on PSH-induced cytotoxicity, the selective ARA3 agonist CI-IB-MECA (15 μM) and the ARA3 antagonist MRS1220 (1 μM) were used in the
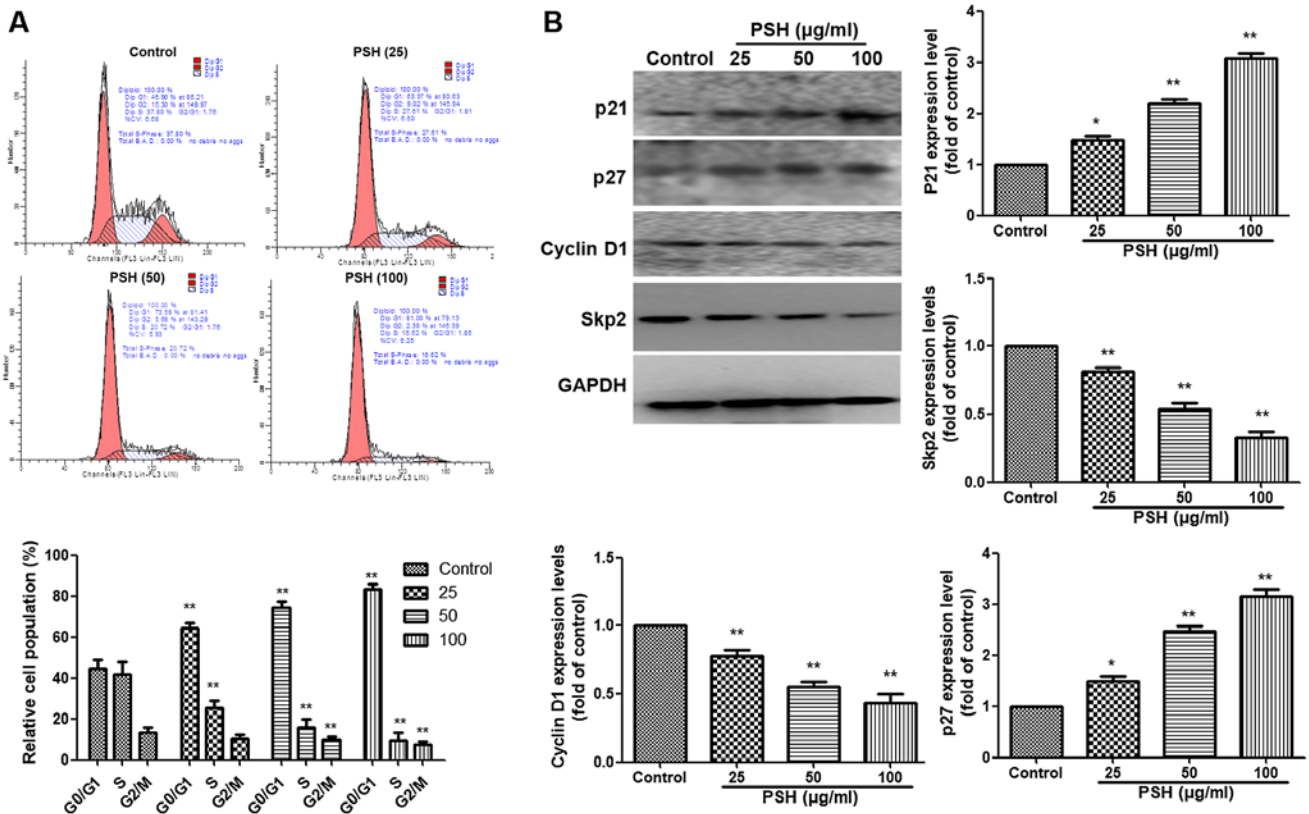
Figure 3. Effects of PSH on the U251 cell cycle. (A) U251 cells were treated with the indicated concentrations of PSH for 48 h, and the cell cycle distribution was determined by flow cytometry using PI staining. (B) The protein expression levels of P21, P27, cyclin D1 and Skp2 were measured by western blotting. The results are presented as the fold-change relative to the control group. Experiments were repeated three times, and the data are presented as the mean ± SD. *$P<0.05$ and **$P<0.01$ vs. control. PSH, *Paris* saponin H; Skp2, S-phase kinase associated protein 2.

subsequent experiments. The inhibitory effects of PSH on the protein expression levels of ARA3, HIF-1α, VEGF, P-Akt, P-44/42 MAPK, cleaved-caspase-3 and cytochrome *c* were abolished by CI-IB-MECA and enhanced by MRS1220 treatment (Fig. 7B). The effects of PSH on cell viability (Fig. 7C) and apoptosis (Fig. 7D) were also reversed by treatment with CI-IB-MECA and enhanced by MRS1220 in U251 cells. These results suggested that the effects of PSH on U251 cells were exerted via the inhibition of ARA3 activity.

Discussion

Glioblastoma is one of the most common and malignant brain tumors (25,26). Common clinical treatments for glioblastoma include surgery, chemotherapy and radiotherapy; however, their therapeutic effects are poor, and the median survival time of patients with glioblastoma is only 6-14 months (3,27). Glioblastomas are resistant to the currently used chemotherapeutic strategies, thus limiting their efficacy (28). Traditional Chinese medicine has been used for thousands of years, and its anticancer effects have attracted increasing attention among pharmacists and scientists (29). Saponins from herbs such as RP possess anticancer activities (30); however, the molecular mechanisms underlying their effects are largely unknown.

Previous studies have demonstrated that the crude extracts from RP and saponins exert inhibitory effects on tumor cell proliferation and progression (31,32). Results from a structure-activity relationship analysis have revealed that the

variety at the C-3 position of the aglycone contributes to the antitumor effects of saponins from RP (19). Previous studies have suggested that polyphyllin D exerts inhibitory effects on tumor cell proliferation and angiogenesis (33-35). By screening the antitumor activity of RP saponins on U87 and U251 glioblastoma cells, it was observed that PSH exhibited the strongest antiglioma effects (data not shown). However, the antitumor activity of PSH and its possible mechanism have remained largely unknown to date. Therefore, the present study verified the anticancer effect of PSH and elucidated the underlying mechanisms.

In the present study, the results of the CCK-8 viability assay demonstrated that PSH inhibited cell viability, and 100 µg/ml PSH reduced U251 cell viability to 60% of that in untreated cells. The effects of PSH on cell migration and invasion were examined by wound healing and Transwell invasion assays, respectively, and the results demonstrated that PSH inhibited U251 cell migration and invasion. These results suggested that PSH exhibited anticancer effects in the U251 glioma cell line. The anticancer effects of PSH may be exerted through several mechanisms, such as cell cycle progression interference and apoptosis promotion. When U251 cells were exposed to PSH in the present study, the apoptotic rates were measured by Annexin V/PI assay, and the results demonstrated that the numbers of apoptotic cells were increased in the PSH treatment groups compared with those in the control group. ELISA results also revealed that the caspase-3 and caspase-9 levels were significantly increased in U251 cells following
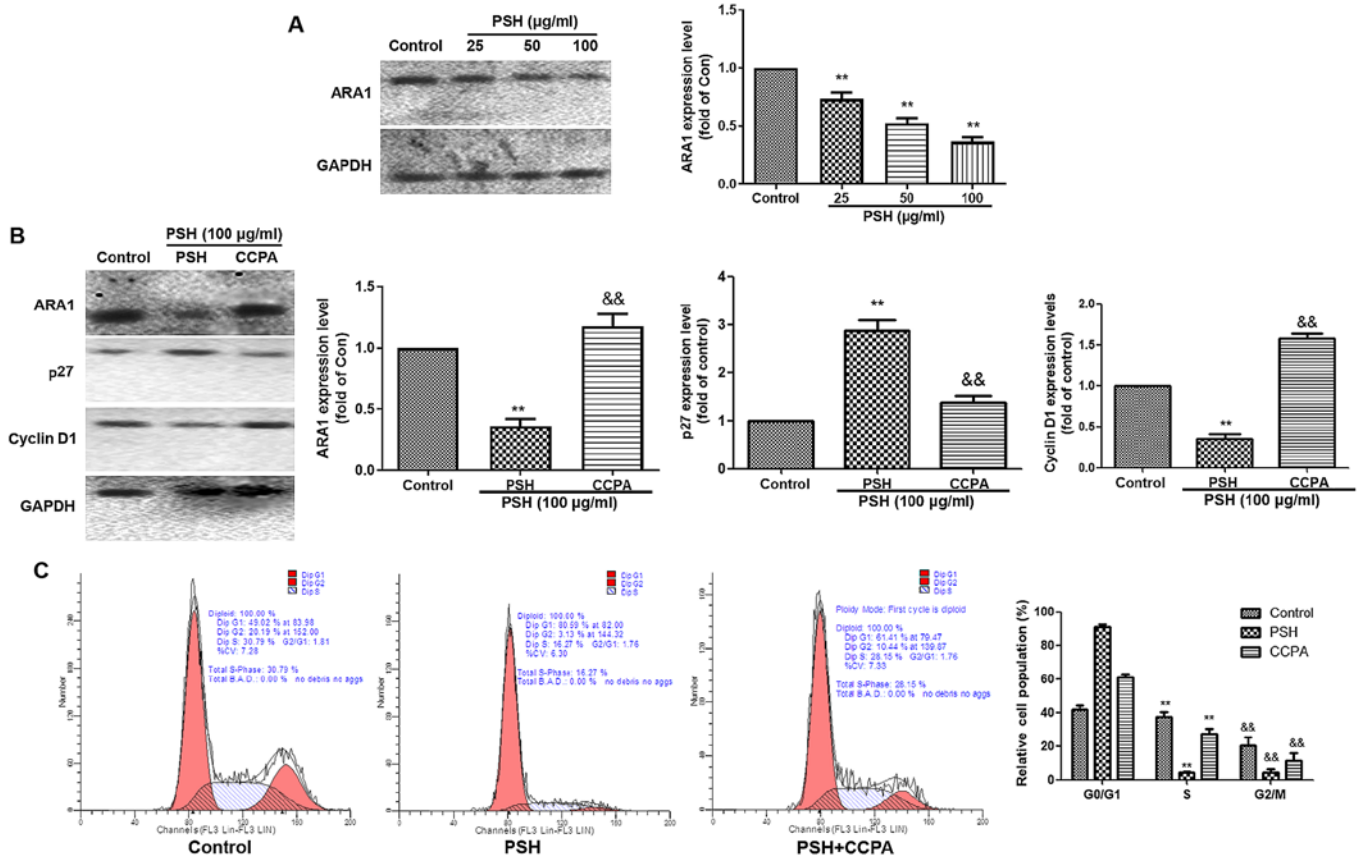
Figure 4. PSH-induced cell cycle arrest is ARA1-dependent. (A) The protein expression levels of ARA1 were measured by western blotting. (B) U251 cells were treated with 20 nM CCPA and 100 µg/ml PSH for 48 h, and the protein expression levels of ARA1, P27 and cyclin D were measured by western blotting. (C) The cell cycle was analyzed by flow cytometry using PI staining. Experiments were repeated three times, and the data are presented as the mean ± SD. **P<0.01 vs. control; &&P<0.01 vs. PSH. PSH, *Paris* saponin H; ARA1, A1 adenosine receptor; CCPA, 2-chloro-N6-cyclopentyladenosine.
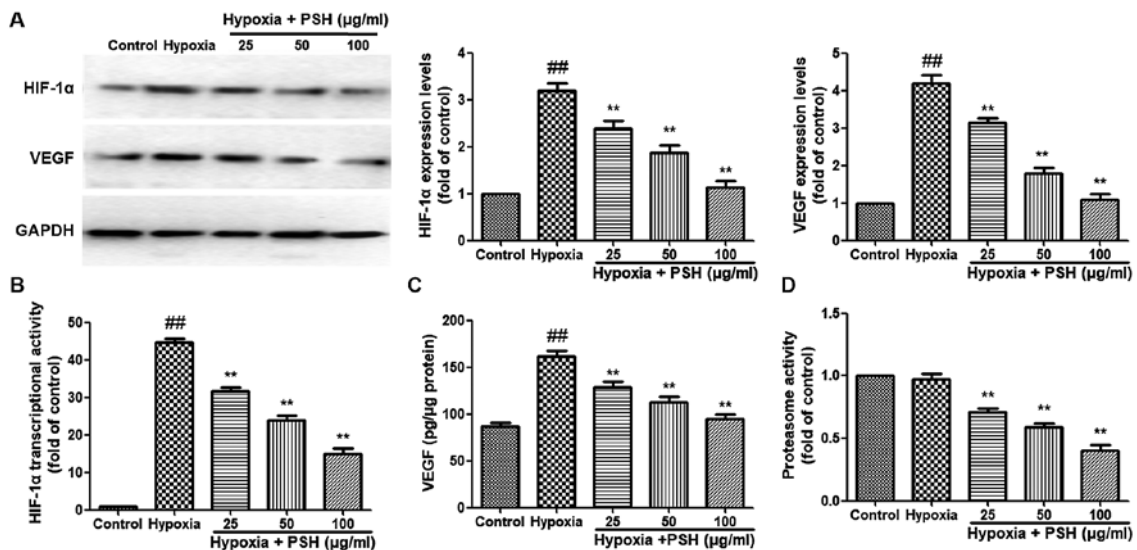

Figure 5. Effects of PSH on the HIF-1α and VEGF expression levels in U251 cells under hypoxia. (A) Protein expression levels of HIF-1α and VEGF in U251 cells. (B) The HIF-1α transcriptional activity was measured by a luciferase reporter assay. The results are presented as the fold-change relative to the control group. (C) PSH inhibited the secretion of VEGF measured by ELISA. (D) PSH inhibited the 20S proteasome activity. Total lysates were isolated and the proteasome activity was measured using a fluorogenic assay kit. Experiments were repeated three times, and the data are presented as the mean ± SD. ##P<0.01 vs. control; **P<0.01 vs. hypoxia. PSH, *Paris* saponin H; HIF-1α, hypoxia-inducible factor-1α; VEGF, vascular endothelial growth factor.

PSH treatment compared with those in the untreated cells, suggesting that PSH may induce caspase-dependent apoptosis in U251 cells. Further western blotting results demonstrated that PSH induced the protein expression of apoptosis-related proteins cleaved caspase-3, cleaved caspase-9, Bax and cytochrome *c*.
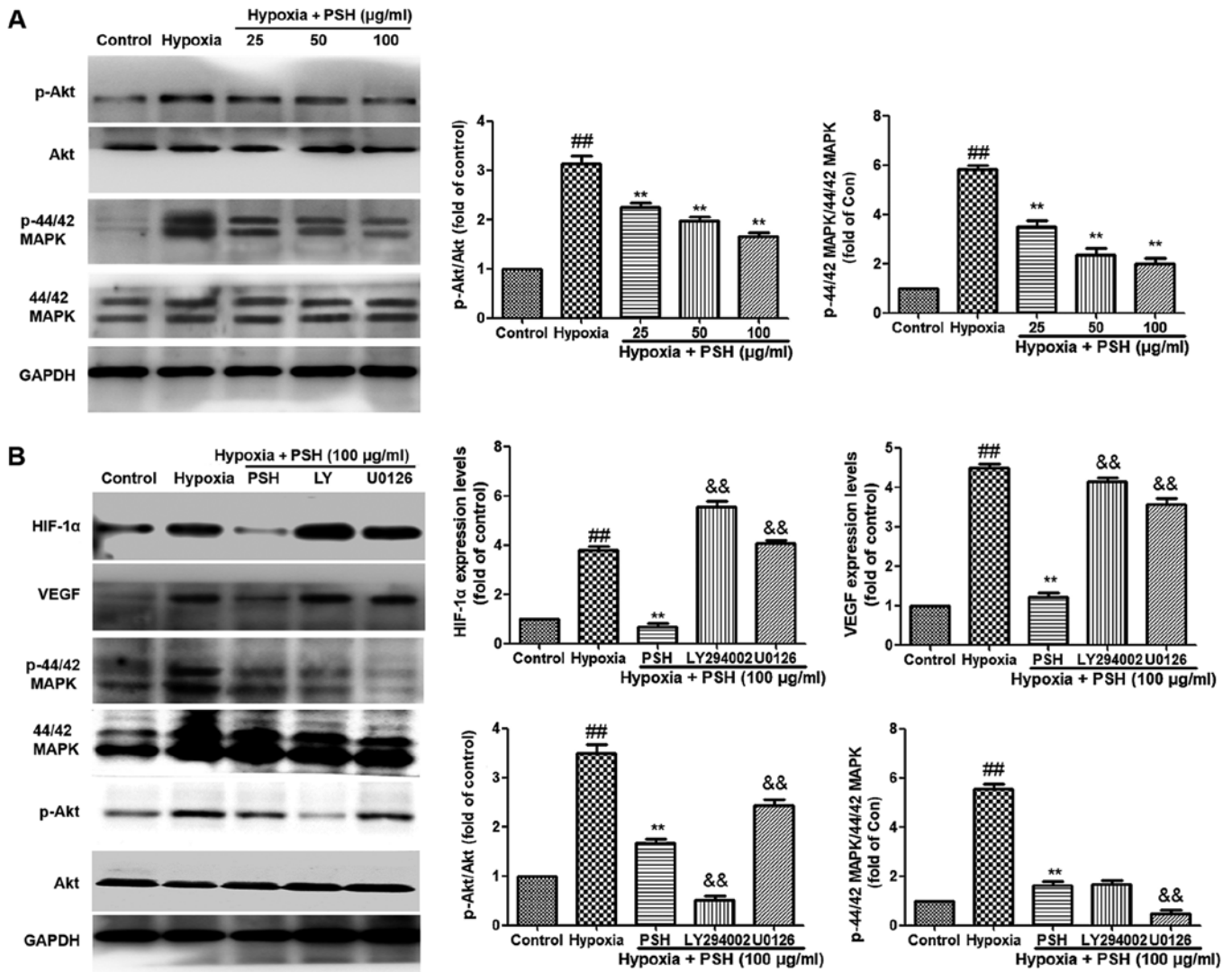
Figure 6. Effects of PSH on PI3K/Akt and 44/42 MAPK phosphorylation levels in U251 cells under hypoxia. (A) PSH inhibited the phosphorylation of PI3K/Akt and 44/42 MAPK. (B) U251 cells were co-treated with 100 μg/ml PSH and 20 μM LY294002 or U0126 for 48 h, and the protein expression levels of HIF-1α, VEGF, 44/42 MAPK and Akt were determined by western blotting. Experiments were repeated three times, and the data are presented as the mean ± SD. [##]P<0.01 vs. control; [**]P<0.01 vs. hypoxia; [&&]P<0.01 vs. PSH. PSH, *Paris* saponin H; MAPK, mitogen-activated protein kinase; HIF-1α, hypoxia-inducible factor-1α; VEGF, vascular endothelial growth factor; P-, phosphorylated.

Cell cycle checkpoints prevent cells from genome damage by undergoing DNA replication or mitosis (36). Interfering with the cell cycle progression is a potentially effective treatment strategy for inhibiting cancer cell proliferation (37). Cell cycle progression is promoted by cyclins D1, D2 and D3, which serve important roles in the modulation of the transition from the G1 to the S phase during the cell cycle, and CDKs, and inhibited by CDK inhibitors, such as p21 and p27 (38,39). The results of the present study demonstrated that PSH induced cell cycle arrest at the G1 phase, increased p21 and p27 protein expression levels, and decreased those of cyclin D1 and Skp2 compared with those in the untreated cells. These results suggested that DNA synthesis in U251 cells was inhibited by PSH.

A previous study has reported that, in the peritumoral area of C6 glioma cell-injected animals, the levels of ARA1 were significantly upregulated compared with those in normal tissues (40). Although the regulatory mechanism of the ARA1 increase is unknown, the levels of ARA1 around tumors represent a useful diagnostic and prognostic marker for glioblastoma

progression (41). To determine whether ARA1 was involved in the PSH-induced cell cycle arrest, the expression levels of ARA1 were analyzed in the present study. The results demonstrated that compared with those in the control group, PSH significantly inhibited the expression levels of ARA1. The ARA1 agonist CCPA was used to verify these results; CCPA treatment abolished the effects of PSH on the cell cycle and the related protein expression. These results suggested that PSH induced U251 cell cycle progression potentially by inhibiting ARA1.

Previous studies have reported that hypoxia is prevalent in solid tumor and hypoxic microenvironments, contributing to radiotherapy resistance (42,43). HIF-1, a transcriptional activator, serves an important role in adapting to low oxygen and nutrition conditions, and promotes tumor progression by regulating the expression of a number of genes, such as AKT and MAPK, involved in angiogenesis, apoptosis, invasion and cell metabolism (44,45). HIF-1 contains two subunits, HIF-1α and HIF-1β. HIF-1α is activated by hypoxia and translocates into the nucleus, where it forms a heterodimer with HIF-1β,
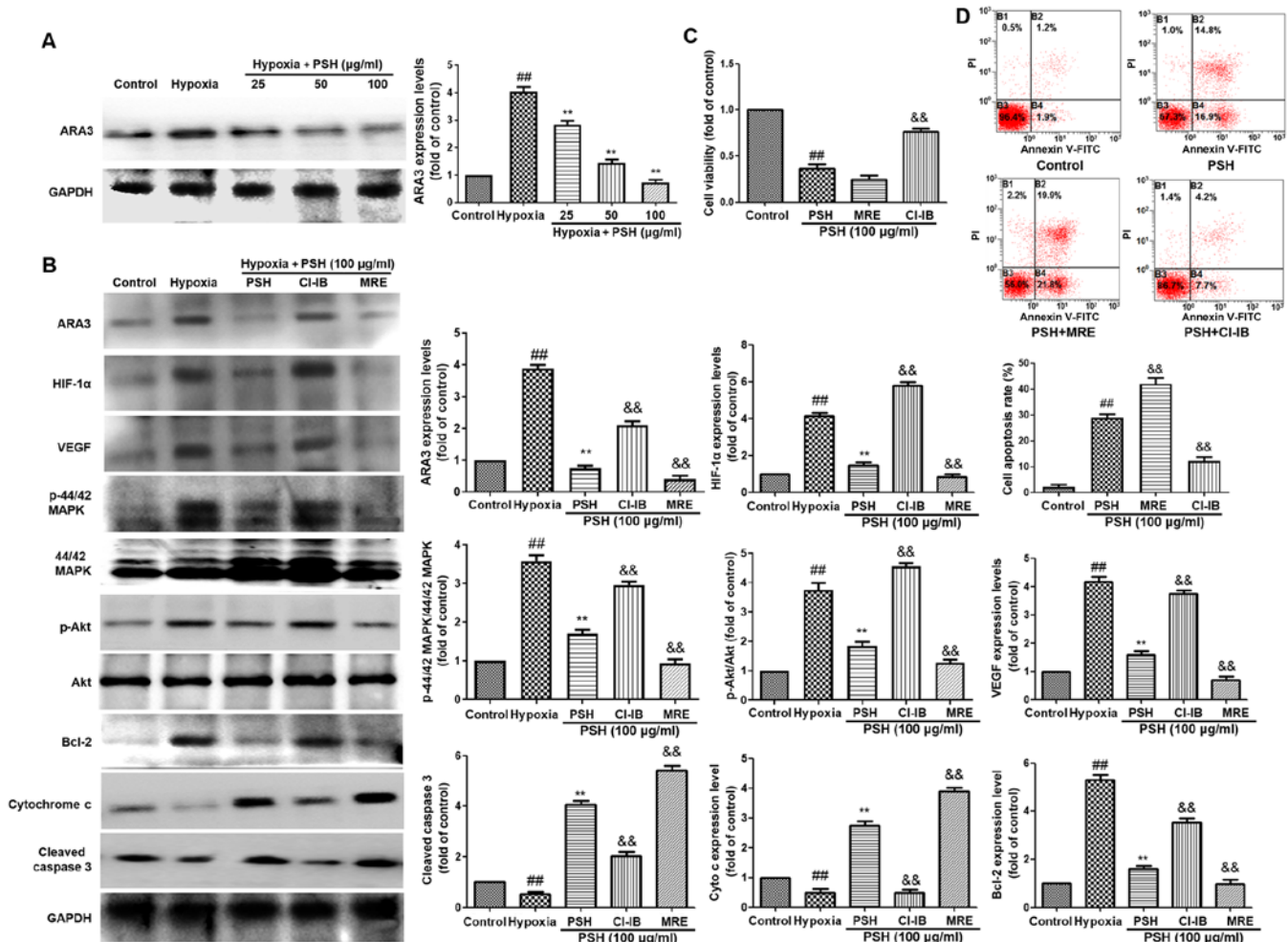
Figure 7. Effects of PSH on U251 cells are partly exerted through the inhibition of ARA3. (A) PSH inhibited the protein expression levels of ARA3. (B) cells were treated with CI-IB-MECA or MRS1220 together with PSH for 48 h, and the protein was isolated for western blotting. Effects of 48-h co-treatment with 15 μM CI-IB-MECA or 1 μM MRS1220 and 100 μg/ml PSH on U251 cell (C) viability and (D) apoptotic rate. Experiments were repeated three times, and the data are presented as the mean $\pm$ SD. [##]P<0.01 vs. control; [**]P<0.01 vs. hypoxia; [&&]P<0.01 vs. PSH. PSH, *Paris* saponin H; CI-IB-MECA, 2-chloro-N6-(3-iodobenzyl) adenosine-50-N-methylcarboxamide; MRS1220, 9-chloro-2-(2-furanyl)-5-(phenylacetyl) amino-(1,2,4) triazolo (1,5-c) quinazoline; ARA3, A3 adenosine receptor.

inducing the expression of a range of transcription factors, including VEGF (46). In the present study, hypoxia upregulated the expression levels of HIF-1α and VEGF in U251 cells compared with those under normoxia. PSH significantly reversed these effects. The 20S proteasome activity was also decreased by PSH treatment compared with that in the hypoxia group. These results suggested that PSH inhibited U251 cell proliferation by regulating HIF-1α and VEGF expression.

HIF-1α is activated by several oncogenic pathways, including phosphatase and tensin homolog (PTEN), as well as growth factors, such as hepatocyte growth factor (HGF) and stromal-derived factor-1a (SDF-1a) (47,48). PTEN negatively regulates Akt expression, which can increase HIF-1α protein synthesis and induce VEGF production under hypoxia (49). P44/42 (also termed ERK1/2), which is a member of the MAPK signaling pathway, activates HIF-1α by promoting the formation of the HIF-p300/CBP complex and modulating its transactivation activity (50). P44/42 MAPK also increases the HIF-1 transcriptional activity by directly phosphorylating HIF-1α (51). P44/42 MAPK induces HIF-1 activation by inhibiting the chromosomal maintenance 1-dependent nuclear export of HIF-1α (52). To determine through which pathway

PSH was involved in controlling HIF-1α, the phosphorylation levels of PI3K/Akt and P44/42 MAPK were analyzed in the present study. The results demonstrated that PSH inhibited the phosphorylation levels of PI3K/Akt and P44/42 MAPK. The specific PI3K/Akt inhibitor LY294002 and P44/42 MAPK inhibitor U0126 were further used to confirm these results; LY294002 and U0126 abolished the inhibitory effects of PSH on the protein expression levels of HIF-1α and VEGF. These results suggested that PSH-mediated inhibition of HIF-1α and VEGF expression was possibly dependent on the PI3K/Akt and p44/42 MAPK pathways.

Under normal conditions, ARA3 inhibits protein kinase A (PKA) and Akt, and activates glycogen synthase kinase 3β, which inhibits tumor cell proliferation (53). However, under hypoxic conditions, ARA3 is activated and upregulates the expression levels of HIF-1α and VEGF, which induces angiogenesis (54). Hypoxia-induced chemoresistance of glioblastoma cells depends on the activation of ARA3, which subsequently induces Akt activation and the inactivation of the pro-apoptotic protein Bad, leading to cell survival (55). In U87 cells, the activation of ARA3 also induces the upregulation of matrix metalloproteinase-9, which increases tumor cell

migration (56). In the present study, the results demonstrated that hypoxia induced, whereas PSH inhibited the expression of ARA3. CI-IB-MECA and MRS1220 were used to confirm the role of ARA3 in PSH treatment; the results revealed that the inhibitory effects of PSH on ARA3, HIF-1α, VEGF, P-Akt, P-44/42 MAPK, cleaved-caspase-3 and cytochrome c expression as well as cell viability were abolished by CI-IB-MECA and enhanced by MRS1220. These results suggested that the effects of PSH were exerted through the inhibition of the ARA3 activity.

Taken together, the results of the present study demonstrated that PSH inhibited the viability and induced cell cycle arrest and apoptosis in U251 cells. The effects of PSH may involve the modulation of adenosine receptor interaction via the inhibition of the P44/42 MAPK and Akt pathways.

Acknowledgements

Availability of data and materials

The datasets used and/or analyzed during the current study are available from the corresponding author on reasonable request.

Authors' contributions

LB and HT designed the study. LB, YLiu1, QY, XZ, YLiu2 and HL performed the study. LB, YLu and JL analyzed the data. LB and HT confirmed the authenticity of all the raw data. LB wrote the manuscript. HT revised the manuscript. All authors read and approved the final manuscript.

Ethics approval and consent to participate

Not applicable.

Patient consent for publication

Not applicable.

Competing interests

The authors declare that they have no competing interests.

References

1. Ordys BB, Launay S, Deighton RF, McCulloch J and Whittle IR: The role of mitochondria in glioma pathophysiology. Mol Neurobiol 42: 64-75, 2010.
2. Batash R, Asna N, Schaffer P, Francis N and Schaffer M: Glioblastoma multiforme, diagnosis and treatment; recent literature review. Curr Med Chem 24: 3002-3009, 2017.
3. de Almeida Sassi F, Lunardi Brunetto A, Schwartsmann G, Roesler R and Abujamra AL: Glioma revisited: From neurogenesis and cancer stem cells to the epigenetic regulation of the niche. J Oncol 2012: 537861, 2012.
4. Yang L, Lin C, Wang L, Guo H and Wang X: Hypoxia and hypoxia-inducible factors in glioblastoma multiforme progression and therapeutic implications. Exp Cell Res 318: 2417-2426, 2012.
5. Shahar T, Nossek E, Steinberg DM, Rozovski U, Blumenthal DT, Bokstein F, Sitt R, Freedman S, Corn BW, Kanner AA and Ram Z: The impact of enrollment in clinical trials on survival of patients with glioblastoma. J Clin Neurosci 19: 1530-1534, 2012.
6. Patil SA, Hosni-Ahmed A, Jones TS, Patil R, Pfeffer LM and Miller DD: Novel approaches to glioma drug design and drug screening. Expert Opin Drug Discov 8: 1135-1151, 2013.
7. Torres Á, Erices JI, Sanchez F, Ehrenfeld P, Turchi L, Virolle T, Uribe D, Niechi I, Spichiger C, Rocha JD, *et al*: Extracellular adenosine promotes cell migration/invasion of glioblastoma stem-like cells through A$_3$ adenosine receptor activation under hypoxia. Cancer Lett 446: 112-122, 2019.
8. Melani A, De Micheli E, Pinna G, Alfieri A, Corte LD and Pedata F: Adenosine extracellular levels in human brain gliomas: An intraoperative microdialysis study. Neurosci Lett 346: 93-96, 2003.
9. Fredholm BB, IJzerman AP, Jacobson KA, Klotz KN and Linden J: International union of pharmacology. XXV. Nomenclature and classification of adenosine receptors. Pharmacol Rev 53: 527-552, 2001.
10. Castillo CA, León D, Ruiz MA, Albasanz JL and Martín M: Modulation of adenosine A1 and A2A receptors in C6 glioma cells during hypoxia: Involvement of endogenous adenosine. J Neurochem 105: 2315-2329, 2008.
11. Wang XY, Chen XL, Tang HF, Gao H, Tian XR and Zhang PH: Cytotoxic triterpenoid saponins from the rhizomes of *Anemone taipaiensis*. Planta Med 77: 1550-1554, 2011.
12. Wang XY, Gao H, Zhang W, Li Y, Cheng G, Sun XL and Tang HF: Bioactive oleanane-type saponins from the rhizomes of *Anemone taipaiensis*. Bioorg Med Chem Lett 23: 5714-5720, 2013.
13. Ji C, Cheng G, Tang H, Zhang Y, Hu Y, Zheng M and Fei Z: Saponin 6 of *Anemone taipaiensis* inhibits proliferation and induces apoptosis of U87 MG cells. Xi Bao Yu Fen Zi Mian Yi Xue Za Zhi 31: 484-486, 2015 (In Chinese).
14. Zhang W, Zhang D, Ma X, Liu Z, Li F and Wu D: Paris saponin VII suppressed the growth of human cervical cancer Hela cells. Eur J Med Res 19: 41, 2014.
15. Zhang T, Liu H, Liu XT, Xu DR, Chen XQ and Wang Q: Qualitative and quantitative analysis of steroidal saponins in crude extracts from *Paris polyphylla* var. yunnanensis and P. polyphylla var. chinensis by high performance liquid chromatography coupled with mass spectrometry. J Pharm Biomed Anal 51: 114-124, 2010.
16. Sun J, Liu BR, Hu WJ, Yu LX and Qian XP: In vitro anticancer activity of aqueous extracts and ethanol extracts of fifteen traditional Chinese medicines on human digestive tumor cell lines. Phytother Res 21: 1102-1104, 2007.
17. Negi JS, Bisht VK, Bhandari AK, Bhatt VP, Singh P and Singh N: Paris polyphylla: Chemical and biological prospectives. Anticancer Agents Med Chem 14: 833-839, 2014.
18. Pang D, Li C, Yang C, Zou Y, Feng B, Li L, Liu W, Geng Y, Luo Q, Chen Z and Huang C: Polyphyllin VII promotes apoptosis and autophagic cell death via ROS-inhibited AKT activity, and sensitizes glioma cells to temozolomide. Oxid Med Cell Longev 2019: 1805635, 2019.
19. Yu Q, Li Q, Lu P and Chen Q: Polyphyllin D induces apoptosis in U87 human glioma cells through the c-Jun NH2-terminal kinase pathway. J Med Food 17: 1036-1042, 2014.
20. Xiao X, Yang M, Xiao J, Zou J, Huang Q, Yang K, Zhang B, Yang F, Liu S, Wang H and Bai P: Paris saponin II suppresses the growth of human ovarian cancer xenografts via modulating VEGF-mediated angiogenesis and tumor cell migration. Cancer Chemother Pharmacol 73: 807-818, 2014.
21. Cong Y, Liu X, Kang L, Yu Z, Zhao Z, Li J, Ma B and Cong Y: Pennogenin tetraglycoside stimulates secretion-dependent activation of rat platelets: Evidence for critical roles of adenosine diphosphate receptor signal pathways. Thromb Res 129: e209-e216, 2012.
22. Cohen FR, Lazareno S and Birdsall NJ: The effects of saponin on the binding and functional properties of the human adenosine A1 receptor. Br J Pharmacol 117: 1521-1529, 1996.
23. Xie X, Zhu H, Zhang J, Wang M, Zhu L, Guo Z, Shen W and Wang D: Solamargine inhibits the migration and invasion of HepG2 cells by blocking epithelial-to-mesenchymal transition. Oncol Lett 14: 447-452, 2017.

24. D'Agostino A, Stellavato A, Busico T, Papa A, Tirino V, Papaccio G, La Gatta A, De Rosa M and Schiraldi C: In vitro analysis of the effects on wound healing of high- and low-molecular weight chains of hyaluronan and their hybrid H-HA/L-HA complexes. BMC Cell Biol 16: 19, 2015.

25. Crocetti E, Trama A, Stiller C, Caldarella A, Soffietti R, Jaal J, Weber DC, Ricardi U, Slowinski J and Brandes A; RARECARE working group: Epidemiology of glial and non-glial brain tumours in Europe. Eur J Cancer 48: 1532-1542, 2012.

26. Ricard D, Idbaih A, Ducray F, Lahutte M, Hoang-Xuan K and Delattre JY: Primary brain tumours in adults. Lancet 379: 1984-1996, 2012.

27. Trembath DG, Lal A, Kroll DJ, Oberlies NH and Riggins GJ: A novel small molecule that selectively inhibits glioblastoma cells expressing EGFRvIII. Mol Cancer 6: 30, 2007.

28. Frosina G: DNA repair and resistance of gliomas to chemotherapy and radiotherapy. Mol Cancer Res 7: 989-999, 2009.

29. Ma L, Wen S, Zhan Y, He Y, Liu X and Jiang J: Anticancer effects of the Chinese medicine matrine on murine hepatocellular carcinoma cells. Planta Med 74: 245-251, 2008.

30. Huang MY, Zhang LL, Ding J and Lu JJ: Anticancer drug discovery from Chinese medicinal herbs. Chin Med 13: 35, 2018.

31. Liu GX, Wang TT, Hu WJ, Qian XP, Yu LX and Liu BR: Anticancer effect of Rhizoma Paridis on primary cancer cells isolated from malignant pleural effusion and ascites. Pract Geriatr 22: 101, 2008.

32. Li X, Wang JH and Xiao YX: Effect of paridis extract on proliferation of human colon cancer SW480 cells and mechanism of the effect. Chin J Biol 23: 619-622+632, 2010.

33. Chan JY, Koon JC, Liu X, Detmar M, Yu B, Kong SK and Fung KP: Polyphyllin D, a steroidal saponin from Paris polyphylla, inhibits endothelial cell functions in vitro and angiogenesis in zebrafish embryos in vivo. J Ethnopharmacol 137: 64-69, 2011.

34. Xiao X, Bai P, Bui Nguyen TM, Xiao J, Liu S, Yang G, Hu L, Chen X, Zhang X, Liu J and Wang H: The antitumoral effect of Paris saponin I associated with the induction of apoptosis through the mitochondrial pathway. Mol Cancer Ther 8: 1179-1188, 2009.

35. Man SL, Wang YL, Li YY, Gao WY, Huang XX and Ma CY: Phytochemistry, pharmacology, toxicology, and structure-cytotoxicity relationship of paridis rhizome saponin. Chin Herbal Med 5: 33-46, 2013.

36. Shackelford RE, Kaufmann WK and Paules RS: Cell cycle control, checkpoint mechanisms, and genotoxic stress. Environ Health Perspect 107 (Suppl 1): S5-S24, 1999.

37. Mork C, Faller D and Spanjaard R: A mechanistic approach to anticancer therapy: Targeting the cell cycle with histone deacetylase inhibitors. Curr Pharm Des 11: 1091-1104, 2005.

38. Evron E, Umbricht CB, Korz D, Raman V, Loeb DM, Niranjan B, Buluwela L, Weitzman SA, Marks J and Sukumar S: Loss of cyclin D2 expression in the majority of breast cancers is associated with promoter hypermethylation. Cancer Res 61: 2782-2787, 2001.

39. Harper JW, Elledge SJ, Keyomarsi K, Dynlacht B, Tsai LH, Zhang P, Dobrowolski S, Bai C, Connell-Crowley L, Swindell E, et al: Inhibition of cyclin-dependent kinases by p21. Mol Biol Cell 6: 387-400, 1995.

40. Dehnhardt M, Palm C, Vieten A, Bauer A and Pietrzyk U: Quantifying the A1AR distribution in peritumoural zones around experimental F98 and C6 rat brain tumours. J Neurooncol 85: 49-63, 2007.

41. Stone TW, Ceruti S and Abbracchio MP: Adenosine receptors and neurological disease: Neuroprotection and neurodegeneration. Handb Exp Pharmacol 45: 535-587, 2009.

42. Thienpont B, Steinbacher J, Zhao H, D'Anna F, Kuchnio A, Ploumakis A, Ghesquière B, Van Dyck L, Boeckx B, Schoonjans L, et al: Tumour hypoxia causes DNA hypermethylation by reducing TET activity. Nature 537: 63-68, 2016.

43. Badowska-Kozakiewicz AM, Sobol M and Patera J: Expression of multidrug resistance protein P-glycoprotein in correlation with markers of hypoxia (HIF-1α, EPO, EPO-R) in invasive breast cancer with metastasis to lymph nodes. Arch Med Sci 13: 1303-1314, 2017.

44. Semenza GL: Regulation of cancer cell metabolism by hypoxia-inducible factor 1. Semin Cancer Biol 19: 12-16, 2009.

45. Veschini L, Belloni D, Foglieni C, Cangi MG, Ferrarini M, Caligaris-Cappio F and Ferrero E: Hypoxia-inducible transcription factor-1 alpha determines sensitivity of endothelial cells to the proteosome inhibitor bortezomib. Blood 109: 2565-2570, 2007.

46. Boddy JL, Fox SB, Han C, Campo L, Turley H, Kanga S, Malone PR and Harris AL: The androgen receptor is significantly associated with vascular endothelial growth factor and hypoxia sensing via hypoxia-inducible factors HIF-1a, HIF-2a, and the prolyl hydroxylases in human prostate cancer. Clin Cancer Res 11: 7658-7663, 2005.

47. Ceradini DJ, Kulkarni AR, Callaghan MJ, Tepper OM, Bastidas N, Kleinman ME, Capla JM, Galiano RD, Levine JP and Gurtner GC: Progenitor cell trafficking is regulated by hypoxic gradients through HIF-1 induction of SDF-1. Nat Med 10: 858-864, 2004.

48. Kitajima Y, Ide T, Ohtsuka T and Miyazaki K: Induction of hepatocyte growth factor activator gene expression under hypoxia activates the hepatocyte growth factor/c-Met system via hypoxia inducible factor-1 in pancreatic cancer. Cancer Sci 99: 1341-1347, 2008.

49. Jiang BH and Liu LZ: PI3K/PTEN signaling in angiogenesis and tumorigenesis. Adv Cancer Res 102: 19-65, 2009.

50. Sang N, Stiehl DP, Bohensky J, Leshchinsky I, Srinivas V and Caro J: MAPK signaling up-regulates the activity of hypoxia-inducible factors by its effects on p300. J Biol Chem 278: 14013-14019, 2003.

51. Richard DE, Berra E, Gothié E, Roux D and Pouysségur J: p42/p44 mitogen-activated protein kinases phosphorylate hypoxia-inducible factor 1alpha (HIF-1alpha) and enhance the transcriptional activity of HIF-1. J Biol Chem 274: 32631-32637, 1999.

52. Mylonis I, Chachami G, Samiotaki M, Panayotou G, Paraskeva E, Kalousi A, Georgatsou E, Bonanou S and Simos G: Identification of MAPK phosphorylation sites and their role in the localization and activity of hypoxia-inducible factor-1alpha. J Biol Chem 281: 33095-33106, 2006.

53. Fishman P, Bar-Yehuda S, Madi L and Cohn I: A3 adenosine receptor as a target for cancer therapy. Anticancer Drugs 13: 437-443, 2002.

54. Merighi S, Benini A, Mirandola P, Gessi S, Varani K, Leung E, Maclennan S and Borea PA: Adenosine modulates vascular endothelial growth factor expression via hypoxia-inducible factor-1 in human glioblastoma cells. Biochem Pharmacol 72: 19-31, 2006.

55. Merighi S, Benini A, Mirandola P, Gessi S, Varani K, Leung E, Maclennan S, Baraldi PG and Borea PA: Hypoxia inhibits paclitaxel-induced apoptosis through adenosine-mediated phosphorylation of bad in glioblastoma cells. Mol Pharmacol 72: 162-172, 2007.

56. Gessi S, Sacchetto V, Fogli E, Merighi S, Varani K, Baraldi PG, Tabrizi MA, Leung E, Maclennan S and Borea PA: Modulation of metalloproteinase-9 in U87MG glioblastoma cells by A3 adenosine receptors. Biochem Pharmacol 79: 1483-1495, 2010.